

# Thermodynamic Performance of a Combined Power and Ejector Refrigeration Cycle

Hyung Jong Ko and Kyoung Hoon Kim

**Abstract**—In this study thermodynamic performance analysis of a combined organic Rankine cycle and ejector refrigeration cycle is carried out for use of low-grade heat source in the form of sensible energy. Special attention is paid to the effects of system parameters including the turbine inlet temperature and turbine inlet pressure on the characteristics of the system such as ratios of mass flow rate, net work production, and refrigeration capacity as well as the coefficient of performance and exergy efficiency of the system. Results show that for a given source the coefficient of performance increases with increasing of the turbine inlet pressure. However, the exergy efficiency has an optimal condition with respect to the turbine inlet pressure.

**Keywords**—Coefficient of performance, ejector refrigeration cycle, exergy efficiency, low-grade energy, organic rankine cycle.

## I. INTRODUCTION

MOST of the low-grade thermal energy is merely discarded, since it is difficult to efficiently convert them into electricity by conventional methods. For the past decades, the organic Rankine cycle (ORC) and the power generating system using binary mixture as a working fluid have attracted much attention as they are proven to be the most feasible methods to achieve high efficiency in converting the low-grade thermal energy to more useful forms of energy [1]-[4].

Velez et al. [5], Raj et al. [6], Tchanche et al. [7], and Chen et al. [8] carried out the review of the state of art of research in energy conversion from low-grade energy sources. Drescher and Bruggemann [9] investigated the ORC in solid biomass power and heat plants. They proposed a method to find suitable thermodynamic fluids for ORCs in biomass plants and found that the family of alkylbenzenes showed the highest efficiency. Schuster et al. [10] mentioned numerous running applications, such as geothermal power plant, biomass fired combined heat and power plants, solar desalination plants, waste heat recovery or micro CHP. Dai et al. [11] used a genetic optimization algorithm, and identified isobutane and R236ea as efficient working fluids. Ho et al. [12] proposed a novel cycle named as organic flash cycle (OFC). In the cycle heat addition occurs with the cycle working fluid remaining in the liquid state, which would ensure near perfect temperature matching to the source stream. Heberle and Bruggemann [13] investigated the

combined heat and power generation for geothermal resources with series and parallel circuits of an ORC.

Low-grade energy sources can be used for the cogeneration of power and refrigeration. This can be achieved by coupling a thermal power cycle with either absorption or ejector refrigeration cycle [14]. Recently, Dai et al. [15] proposed a combined power and refrigeration cycle, which combines the Rankine cycle and the ejector refrigeration cycle. This combined cycle produces both power output and refrigeration output simultaneously and it can be driven by the flue gas of gas turbine or engine, solar energy, geothermal energy and industrial waste heats. Li et al. [16] proposed an organic Rankine cycle with ejector (EORC) for the purpose of increasing the power output capacity and its efficiency. Habibzadeh et al. [17] performed the thermodynamic study of a thermal system which combines an organic Rankine cycle and an ejector refrigeration cycle using classical and finite-size thermodynamics.

In this study the thermodynamic performance of a combined power and ejector refrigeration cycle is carried out for use of low-grade heat source in the form of sensible energy. The effects of the system parameters including the turbine inlet temperature and pressure on the system characteristics such as ratios of mass flow rate, net work production, and refrigeration capacity as well as the coefficient of performance (COP) and exergy efficiency are investigated.

## II. SYSTEM ANALYSIS

The system considered in this work is an organic Rankine cycle combined with an ejector refrigeration cycle and its schematic diagram is shown in Fig. 1. The system consists of a pump, boiler, turbine, ejector, condenser, expansion valve, and evaporator. The working fluid considered in this study is R245fa and its thermodynamic properties are calculated by the Patel-Teja equation of state [18]. The basic data of the working fluid which are needed to apply the Patel-Teja equation are shown in Table I, where  $M$ ,  $T_{cr}$ ,  $P_{cr}$  and  $\omega$  are molecular weight, critical temperature, critical pressure, and acentric factor, respectively [19]. The system is driven by the sensible energy supplied by a low-grade heat source. Heat rejection to the coolant and refrigeration space takes place in the condenser and evaporator, respectively.

TABLE I  
BASIC DATA OF THE WORKING FLUID

Substance	$M$ (kg/kmol)	$T_{cr}$ (K)	$P_{cr}$ (bar)	$\omega$
R245fa	134.048	427.2	36.40	0.3724

Hyung Jong Ko is with the Dept. Mech. Eng., Kumoh National Institute of Technology, 61 Daehak-ro, Gumi, Gyeongbuk 730-701, Korea (e-mail: kohj@kumoh.ac.kr).

Kyoung Hoon Kim is with the Dept. Mech. Eng., Kumoh National Institute of Technology, 61 Daehak-ro, Gumi, Gyeongbuk 730-701, Korea (corresponding author. phone: 82-54-478-7292; fax: 82-54-478-7319; e-mail: khkim@kumoh.ac.kr).

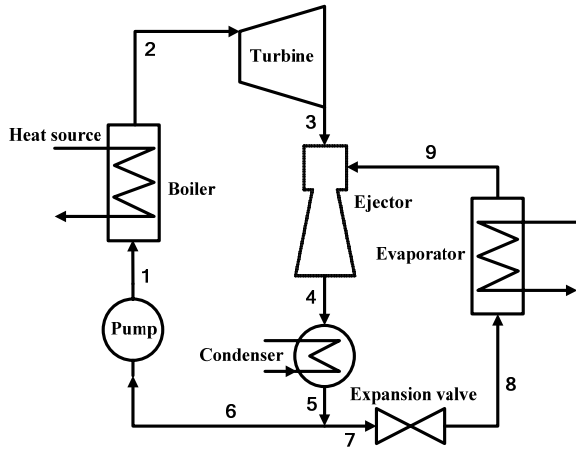


Fig. 1 Schematic diagram of the system

In order to investigate the thermodynamic performance of the system the following simplifications are utilized.

- 1) The source and coolant fluids are water at temperature of  $T_s$  and  $T_c$ , respectively.
- 2) The working fluid enters the turbine as superheated vapor with temperature of  $T_h$  and pressure of  $P_h$ .
- 3) The working fluid leaves the condenser as saturated liquid at temperature of  $T_{cd}$ .
- 4) The minimum temperature difference between the hot and cold streams in the boiler and condenser is held at a prescribed value of pinch point temperature difference,  $\Delta T_{pp}$ .
- 5) Pressure drop and heat loss in the system are negligible.
- 6) The pump and turbine have constant isentropic efficiencies of  $\eta_p$  and  $\eta_t$ , respectively.
- 7) The flow in the ejector is one-dimensional and the velocities at the inlet and outlet are negligible. Mixing of the primary and secondary flows occurs at constant pressure. The effects of irreversibility at the nozzle, mixing, and diffuser sections can be taken into account by using the nozzle, mixing, and diffuser efficiencies of  $\eta_n$ ,  $\eta_m$ , and  $\eta_d$ , respectively [15].

Using these assumptions and referring to Fig. 1 the thermodynamic states at 1 to 9 are determined as follows. The points 1 and 2 are determined using  $P_h$ ,  $\eta_p$  and  $P_h$ ,  $T_h$ , respectively. Similarly the point 3 is determined using the turbine outlet pressure  $P_m$  and  $\eta_t$ . The state at the exit 4 and the entrainment ratio  $r_{e/t}$  of the ejector are determined iteratively using the conservation equations and  $P_m$ , evaporator pressure  $P_e$ , and condenser pressure  $P_{cd}$  and  $\eta_n$ ,  $\eta_m$ , and  $\eta_d$ . It is noted that  $P_e$  is the saturation pressure at the evaporator temperature  $T_e$  and  $r_{e/t}$  is equal to the ratio of mass flow rate of the evaporator to turbine. The working fluids at 5, 6, and 7 are at the same thermodynamic states and are saturated liquids at  $T_{cd}$ . The corresponding saturation pressure defines  $P_{cd}$ . The relations  $P_8 = P_e$  and  $h_8 = h_7$  determine point 8. The exit of evaporator 9 corresponds to the saturated vapor at temperature  $T_e$ .

It is desirable to circulate more working fluid and less coolant fluid for a given mass flow rate of source fluid, unless

the pinch point condition is violated. The ratios of mass flow rate of working fluid and coolant fluid to that of source fluid can be determined from the energy balance and the pinch point condition. Note that the mass flow rate in the condenser is equal to the sum of those in the turbine and evaporator:

$$m_{cd} = m_t + m_e \quad (1)$$

The rates of heat input, net work production and refrigeration output can be calculated from

$$Q_{in} = m_t(h_2 - h_1) \quad (2)$$

$$W_{net} = W_t - W_p = m_t[(h_3 - h_2) - (h_1 - h_6)] \quad (3)$$

$$Q_e = m_e(h_9 - h_8) \quad (4)$$

The rate of exergy input to the system by the source fluid and the exergy output associated with refrigeration can be calculated as

$$E_{in} = m_s c_{ps} \{T_s - T_0 - T_0 \ln(T_s / T_0)\} \quad (5)$$

$$E_e = Q_e(T_0 - T_{cs}) / T_{cs} \quad (6)$$

where the subscript 0 refers to the dead state and  $T_{cs}$  is the temperature of the cooled space.

As the system cogenerates power and refrigeration output, the overall performance of the system can be assessed with the coefficient of performance (COP) and the exergy efficiency  $\eta_{ex}$ . These are defined as follows:

$$COP = (W_{net} + Q_e) / Q_{in} \quad (7)$$

$$\eta_{ex} = (W_{net} + E_e) / E_{in} \quad (8)$$

### III. RESULTS AND DISCUSSIONS

In this study source fluid is water with temperature of  $T_s = 150^\circ\text{C}$ . The performance of the system is parametrically investigated for the varying parameter values. The inlet ( $P_h$ ) and outlet ( $P_m$ ) pressure of turbine are varied from 5 to 20 bar and from 3 to 4 bar, respectively, while the turbine inlet ( $T_h$ ) and condenser ( $T_{cd}$ ) temperature ranging from 100 to  $120^\circ\text{C}$  and from 22 to  $30^\circ\text{C}$  are considered. Other basic data for analysis are as follows;  $T_c = 15^\circ\text{C}$ ,  $T_e = -20^\circ\text{C}$ ,  $T_{cs} = -5^\circ\text{C}$ ,  $\Delta T_{pp} = 10^\circ\text{C}$ ,  $\eta_p = 0.7$ ,  $\eta_t = 0.85$ ,  $\eta_n = 0.95$ ,  $\eta_m = 0.95$ ,  $\eta_d = 0.95$ .

In the combined cycle the power generation performance is mainly influenced by the turbine inlet conditions, while the refrigeration characteristics are affected by the conditions at the turbine outlet and condenser. Therefore the former is investigated by varying  $P_h$  and  $T_h$ , and the latter by varying  $P_m$  and  $T_{cd}$ .

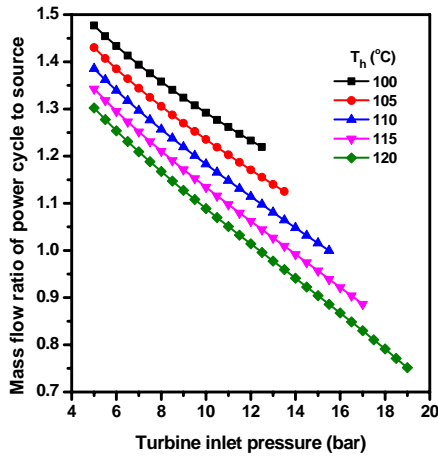


Fig. 2 Dependence of mass flow ratio of power cycle to source on the turbine inlet conditions

Fig. 2 shows the dependence of mass flow ratio of power cycle to source fluid,  $r_{v/s}$ , on the turbine inlet conditions for  $P_m = 3$  bar and  $T_{cd} = 30^\circ\text{C}$ . Turbine inlet pressure is limited such that the working fluid enters turbine as a superheated vapor. For example  $P_h < 12.5$  bar for  $T_h = 100^\circ\text{C}$ .  $r_{v/s}$  is an important variable because it characterizes the performance on a base of unit mass of source fluid. As a high  $P_h$  or  $T_h$  means a big heat load during heating process,  $r_{v/s}$  is lower for higher  $P_h$  or  $T_h$ . The dependence of  $r_{v/s}$  on  $P_h$  is almost linear but the dependence on  $P_m$  or  $T_{cd}$  is weak.

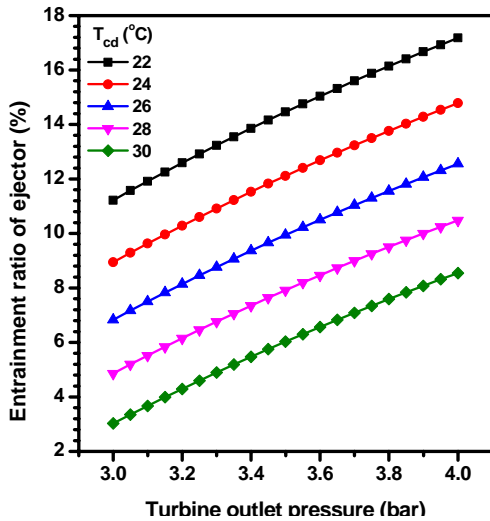


Fig. 3 Dependence of entrainment ratio of ejector on turbine outlet pressure and condenser temperature

Fig. 3 shows the dependence of entrainment ratio of ejector,  $r_{e/t}$ , on turbine outlet pressure and condenser temperature for  $P_h = 10$  bar and  $T_h = 110^\circ\text{C}$ .  $r_{e/t}$  is defined as the ratio of secondary flow rate to primary flow rate in the ejector, and equal to the ratio of mass flow rate in evaporator to that in turbine.  $r_{e/t}$  characterizes the refrigeration performance.  $r_{e/t}$  increases almost linearly with  $P_m$  since high  $P_m$  implies high energy of the primary flow which is needed to entrain the secondary flow.

On the contrary high  $T_{cd}$  lowers entrainment ratio since it means a high back pressure of ejector resulting in a high compression ratio. The dependence of entrainment ratio on the turbine inlet condition is very weak.

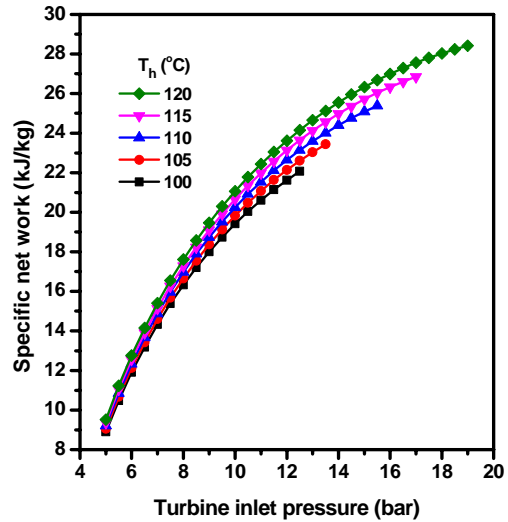


Fig. 4 Dependence of net work per unit mass of working fluid on the turbine inlet conditions

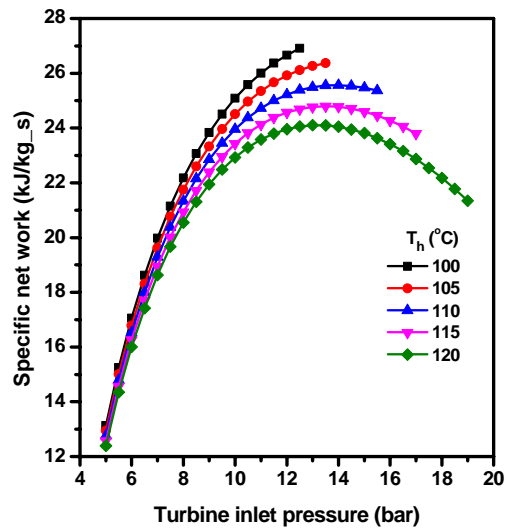


Fig. 5 Dependence of net work per unit mass of source fluid on the turbine inlet conditions

The dependences of the specific net work on the turbine inlet conditions for  $P_m = 3$  bar and  $T_{cd} = 30^\circ\text{C}$  are given for a unit mass of working fluid,  $w_{n/t} = W_{net}/m_t$ , in Fig. 4 and for a unit mass of source fluid,  $w_{n/s} = W_{net}/m_s$ , in Fig. 5, respectively. Note a relation  $w_{n/s} = w_{n/t} r_{v/s}$ . For the pressure range considered,  $w_{n/t}$  increases with  $P_h$  and  $T_h$ , which can be readily expected since the enthalpy drop increases with them for fixed  $P_m$ . For fixed  $T_h$ , the dependence of  $w_{n/s}$  on  $P_h$  is similar to  $w_{n/t}$  for relatively low  $P_h$  range. However it begins to decrease with  $P_h$  from peak points. Moreover  $w_{n/s}$  is smaller for higher  $T_h$ . These different behaviors may be explained through the factor  $r_{v/s}$  shown in Fig. 2. For a given low-grade energy source more efficient power

generation is expected if the system is operated for the TIP output. giving peak value of  $w_{n/s}$ .

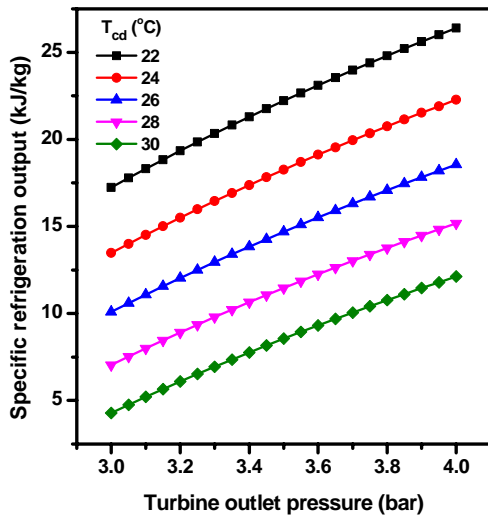


Fig. 6 Refrigeration output per unit mass of working fluid versus turbine outlet pressure and condenser temperature

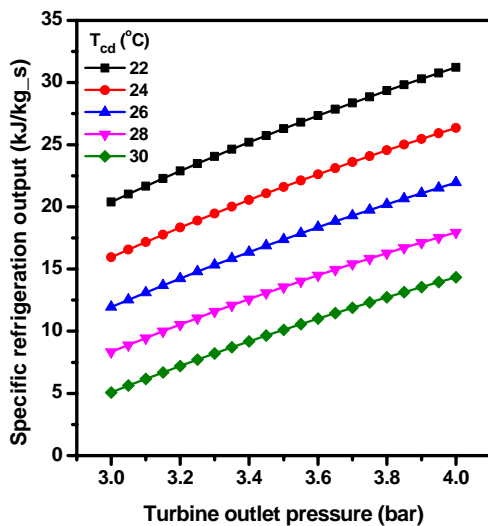


Fig. 7 Refrigeration output per unit mass of source fluid versus turbine outlet pressure and condenser temperature

Figs. 6 and 7 show the dependence of the specific refrigeration output on turbine outlet pressure and condenser temperature for  $P_h = 10$  bar and  $T_h = 110^\circ\text{C}$  for a unit mass of working fluid,  $q_{e/t} = Q_c/m_t$  and for a unit mass of source fluid,  $q_{e/s} = Q_c/m_s$ , respectively. Note that  $q_{e/s}$  is  $q_{e/t}$  multiplied by  $r_{v/s}$ . Contrary to the specific net works,  $q_{e/t}$  and  $q_{e/s}$  show the qualitatively same behavior as the entrainment ratio, because the evaporator temperature is fixed. They increase almost linearly with respect the increase of  $P_m$  and are smaller at higher condenser temperatures. Raising the turbine outlet temperature could give more refrigeration output with a sacrifice of the reduced power generation due to the decrease of enthalpy drop in the turbine. In spite of the low entrainment ratio ranging from 3 to 18%, the refrigeration out is comparable to the power

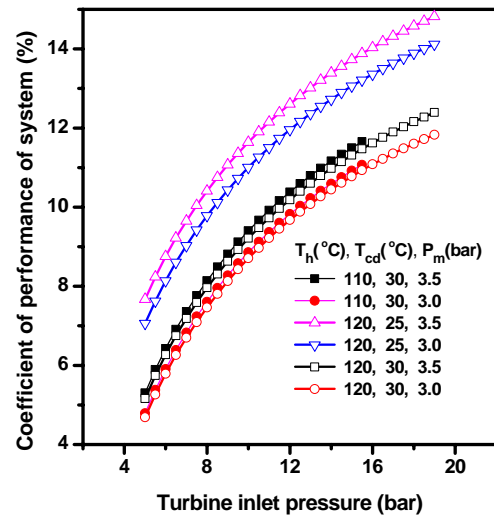


Fig. 8 Variations of the coefficient of performance with respect to the conditions of turbine and condenser

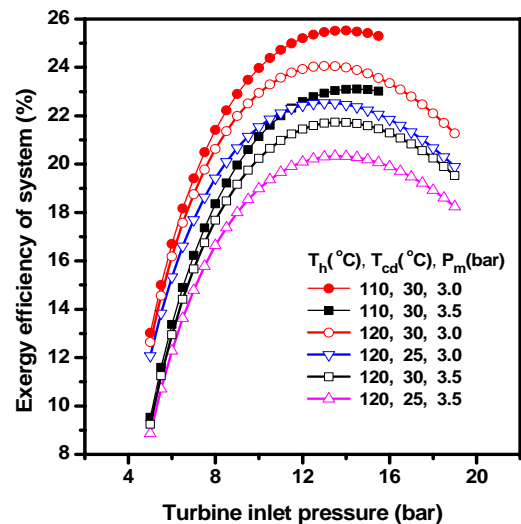


Fig. 9 Variations of the exergy efficiency with respect to the conditions of turbine and condenser

Finally the overall performance of system is investigated in terms of the coefficient of performance ( $COP$ ) and exergy efficiency for the fixed source temperature. Fig. 8 shows the variations of  $COP$  with respect to the conditions of turbine and condenser. For the range of  $P_h$  considered  $COP$  increases with  $P_h$ .  $COP$  is higher for lower  $T_{cd}$  because both power and refrigeration output are larger at lower  $T_{cd}$ . On the while,  $COP$  is higher for higher  $P_m$ , as the increased refrigeration output overweighed the negative effect of reduced enthalpy drop. Although the difference is small  $COP$  is higher for lower  $T_h$ .

Variations of the exergy efficiency with respect to the conditions of turbine and condenser are shown in Fig. 9. In contrast to  $COP$ , exergy efficiency curves show bell shapes with respect to  $P_h$ , which implies the existence of  $P_h$  value for the optimal utilization of given energy source. The exergy

efficiency is higher for lower  $T_h$ , lower  $P_m$ , and higher  $T_{cd}$ , when other parameters are fixed.

#### IV. CONCLUSIONS

In this study, the performance of a combined power and ejector refrigeration cycle is thermodynamically investigated. The main results can be summarized as follows.

- Entrainment ratio of ejector increases almost linearly with turbine outlet pressure and is higher for lower condenser temperature.
- The coefficient of performance increases with turbine inlet pressure and is higher for lower condenser temperature and turbine outlet pressure.
- The exergy efficiency has an optimal condition with respect to turbine inlet pressure for a fixed source temperature. The exergy efficiency is higher for lower turbine inlet temperature, lower turbine outlet pressure, and higher condenser temperature.

#### ACKNOWLEDGMENT

This research was supported by Basic Science Research Program through the National Research Foundation of Korea (NRF) funded by the Ministry of Education, Science and Technology (No. 2012-013929).

#### REFERENCES

- [1] T. C. Hung, T. Y. Shai, and S. K. Wang, "A review of organic Rankine cycles (ORCs) for the recovery of low-grade waste heat," *Energy*, vol. 22, pp. 661-667, 1997.
- [2] N. A. Lai, M. Wendland, and J. Fisher, "Working fluids for high temperature organic Rankine cycle," *Energy*, vol. 36, pp. 199-211, 2011.
- [3] K. H. Kim, C. H. Han, and K. Kim, "Effects of ammonia concentration on the thermodynamic performances of ammonia-water based power cycles," *Thermochimica Acta*, vol. 530, pp. 7-16, 2012.
- [4] K. H. Kim, C. H. Han, and K. Kim, "Comparative exergy analysis of ammonia-water based Rankine cycles with and without regeneration," *Int. J. Exergy*, vol. 16, pp. 344-361, 2013.
- [5] F. Velez, J. J. Segovia, M. C. Martin, G. Antolin, F. Chejne, and A. Quijano, "Comparative study of working fluids for a Rankine cycle operating at low temperature," *Fuel Proc. Tech.*, vol. 103, pp. 71-77, 2012.
- [6] N. T. Raj, S. Iniyar, and R. Goic, "A review of renewable energy based cogeneration technologies," *Renew. Sustain. Energy Rev.*, vol. 15, pp. 3640-3648, 2011.
- [7] B. F. Tchanché, Gr. Lambrinos, A. Frangoudakis, and G. Papadakis, "Low-grade heat conversion into power using organic Rankine cycles - A review of various applications," *Renew. Sustain. Energy Rev.*, vol. 15, pp. 3963-3979, 2011.
- [8] H. Chen, D. Y. Goswami, and E. Stefanakos, "A review of thermodynamic cycles and working fluids for the conversion of low-grade heat," *Renew. Sustain. Energy Rev.*, vol. 14, pp. 3059-3067, 2010.
- [9] U. Drescher and D. Brueggemann, "Fluid selection for the organic Rankine cycle (ORC) in biomass power and heat plants," *Appl. Therm. Eng.*, vol. 27, pp. 223-228, 2007.
- [10] A. Schuster, S. Karellas, and H. Splithoff, "Energetic and economic investigation of innovative Organic Rankine Cycle applications," *Appl. Therm. Eng.*, vol. 29, pp. 1809-1817, 2008.
- [11] Y. Dai, J. Wang, and L. Gao, "Parametric optimization and comparative study of organic Rankine cycle (ORC) for low grade waste heat recovery," *Energy Convs. Mgmt.*, vol. 50, pp. 576-582, 2009.
- [12] T. Ho, S. S. Mao, and R. Greif, "Increased power production through enhancements to the Organic Flash Cycle (OFC)," *Energy*, vol. 45, pp. 686-695, 2012.
- [13] F. Heberle, D. Brueggemann, "Exergy based fluid selection for a geothermal organic Rankine cycle for combined heat and power generation," *Appl. Therm. Eng.*, vol. 30, pp. 1326-1332, 2010.
- [14] G. Demirkaya, R. V. Padilla, D. Y. Goswami, E. Stefanakos, and M. M. Rahman, "Analysis of a combined power and cooling cycle for low-grade heat sources," *Int. J. Energy Res.*, vol. 35, pp. 1145-1157, 2011.
- [15] Y. Dai, J. Wang, and L. Gao, "Exergy analysis, parametric analysis and optimization for a novel combined power and ejector refrigeration cycle," *Appl. Therm. Eng.*, vol. 28, pp. 335-340, 2009.
- [16] X. Li, C. Zhao, and X. Hu, "Thermodynamic analysis of organic Rankine cycle with ejector," *Energy*, vol. 42, pp. 342-349, 2012.
- [17] A. Habibzadeh, M. M. Rashidi, and N. Galanis, "Analysis of a combined power and ejector-refrigeration cycle using low temperature heat," *Energy Convs. Mgmt.*, vol. 65, pp. 381-391, 2013.
- [18] T. Yang, G. J. Chen, and T. M. Guo, "Extension of the Wong-Sandler mixing rule to the three-parameter Peng-Robinson equation of state: Application up to the near-critical region," *Chem. Eng. J.*, vol. 67, pp. 27-36, 1997.
- [19] C. L. Yaws, *Chemical properties handbook*, McGraw-Hill, 1999.